JOURNAL OF Materials CHEMISTRY

XPS study of coating delamination from non-rinse chromate treated steel

Masatsugu Murase[a] **and John F. Watts***[b]

[a]*Kawasaki Steel Corporation, 1 Kawasaki-cho, Chuou-ku, Chiba, 260, Japan*
[b]*School of Mechanical and Materials Engineering, University of Surrey, Guildford, Surrey, UK GU2 5XH*

The mechanisms of delamination of an epoxy coated steel system with various substrate non-rinse chromate treatments has been investigated by XPS and TOF-SIMS. First, the chromate surface before epoxy coating was investigated to establish the layer structure produced by the chromate treatments. The pre-treatment layer was found to be a complex material consisting of trivalent and hexavalent chromium, and a cross-linked structure of these ions within chromium oxide. A non-rinse chromate with colloidal SiO_2 added has a similar structure of trivalent and hexavalent chromium oxide at the outer surface, but within the inner layer Cr oxide and SiO_2 are bonded to each other. This leads to a more complicated structure compared to the chromate treatment. Adsorption isotherms of epoxy resin and curing agent on chromate layers were established by using XPS, in order to evaluate the adsorption characteristics of these molecules, to gain an insight into the initial stages of adhesion. The chromate surface was found to have more bonding sites than the chromate with SiO_2 surface.

Steel substrates treated in this manner were coated with an epoxy coating and exposed to a saline environment at both the free corrosion potential and a cathodic potential The delamination kinetics of the epoxy coating were recorded. Interfacial failure surfaces from the delamination studies were examined by XPS and TOF-SIMS. By obtaining Cr 2p spectra at high resolution and peak-fitting to resolve the chemical states present, it has proved possible to determine the layer structure produced by the chromate treatment and elucidate their chemical behaviour during the electrochemical tests. In the case of the chromate treatment, failure following cathodic polarisation is within the conversion coating itself and associated with the inner layer, whilst an interfacial failure was observed for the untreated bare steel. All failure surfaces of the chromate treated steel sample were rich in Cr^{3+}, compared with the initial value obtained before the delamination experiments, and rich in sodium. It is shown that cathodic conditions exist under epoxy coating which have brought about the reduction of Cr^{6+} to Cr^{3+} within the chromate layer. This cathodic reduction, in the case of the chromate treated sample, leads to failure by the destruction of the cross-linked structure incorporating Cr^{6+} and Cr^{3+}.

Surface pre-treatment plays an important role in the durability of organic coatings. A variety of pre-treatments for organic coatings have been devised over the years that provide excellent durability under wet and humid conditions. Recently, chromate treatments have seen a widespread increase as a pre-treatment used in conjunction with organic coatings in, for example, the automobile industry, marine structures and steel line pipe. As a result of the desire to move to a more environmentally friendly process, by avoiding the need to dispose of waste containing chromium(VI) residues, non-rinse chromate treatments have attracted much attention.[1,2] A fuller understanding of the degradation mechanism of such pretreatments is, however, required.

A most important requirement in understanding the mechanism of organic coating degradation and failure is the definition of the exact locus of failure. Surface analysis techniques such as X-ray photoelectron spectroscopy (XPS) have been used for a number of years by several authors to study the exact locus of failure of various organic coatings.[3] Such studies have tended to concentrate on environmental aspects of coating failure and relate these observations to the observed behaviour, such as durability, of the organic coatings or adhesives.[4,5] Diffusion of aggressive species such as water, oxygen, cations and anions from the environment to the environs of the organic/inorganic interface is known to reduce the level of adhesion and cause coating delamination. Cathodic polarisation, which can be encountered as a result of impressed current or sacrificial cathodic protection, or indeed as a result of discrete anodic and cathodic activity at the exposed metal surface of a defect in a coated substrate[6,7] is known to accelerate the coating delamination. This phenomenon, cathodic delamination, has been identified as a route to failure in the case of steel substrates since the late 1920s. There is, however, still much debate as to the exact mechanism and it seems likely that there is no one unique mechanism.[8–10] Several workers have reported this process, and described the mode of failure of organic coatings applied to steel surfaces and more recently of adhesively bonded zinc coated steel. Little is known, however, about the failure mechanism of organic coatings applied to the new generation of chromate treatments on steel.

In this paper we report the use of XPS and TOF-SIMS to study the interfacial failure surfaces of epoxy coatings applied to steel which has been treated using a non-rinse chromate treatment, and then exposed to an aqueous solution at either the free corrosion potential or at an impressed cathodic potential. The aim of this work is both to deduce the interfacial chemistry of the formation of the chromate treatment and subsequent coatings delamination by using surface analysis methods.

Experimental

Materials

Three kinds of pre-treated and epoxy coated steel sample were used for this study. The substrate material used was 0.8 mm thick cold rolled steel.

The chromate solution was a mixture of hexavalent chromium and trivalent chromium, in the molar ratio of $[Cr^{3+}]/[Cr^{3+}+Cr^{6+}]=0.35$, prepared in the following manner. The chromate solution was prepared from chromium

trioxide solution by adding ethylene glycol as a reducing agent, 0.25 mol of ethylene glycol was added to 1 mol of chromium trioxide and the solution concentration of chromium trioxide was adjusted to 0.2 mol dm^{-3}. As the CrO_3, a strong oxidising agent, is added to excess, the reaction will not go to completion and the residual solution will therefore contain both Cr^{VI}, the residual reactant, and Cr^{III} as the reduced form of the oxidising agent. The reactant concentrations were chosen to yield the required $[Cr^{3+}]/[Cr^{3+}+Cr^{6+}]$ ratio as indicated above. This treatment provided a common coating with the layer structure shown in Fig. 1.

The data reported here relate to the delamination of an organic coating from bare steel, and steel treated with chromate solution and steel treated with a chromate $+SiO_2$ solution. The latter chromate solution was prepared by the addition of 0.28 mol of colloidal SiO_2 to 1 mol of the standard chromate solution, to give a Si/Cr atomic ratio of 1.4. The surface substrate was degreased by dipping in a mild alkaline solution followed by water rinsing, following degreasing the substrate was coated with chromate solution by a roll coater, and oven dried at 140 °C for 3 min. This treatment yielded a chromate coating mass of 150 mg Cr m^{-2}.

The epoxy coating employed was formulated using Epikote 828 (Shell) and an amine curing agent (B002 obtained from Mitsubishi Kasei Corporation), in the molar ratio of 1.00 : 0.67. The epoxy coating was applied by a roll coater to both chromate treated substrates and degreased steel to a wet thickness of 50 μm. After roll coating, samples were heated in an electric oven at 140 °C for 5 min, which gave a dry film thickness of *ca.* 30 μm.

For the direct observation of interface chemistry by XPS very thin coatings of epoxy were required, as described elsewhere.[12] This can be readily achieved by spin coating from a very dilute solution. Spin coated samples were prepared on 10 mm diameter discs of chromate treated steel, using a 2.4×10^{-4} mol dm^{-3} solution of the epoxy/curing agent mixture in toluene. A controlled volume of solution was deposited on the substrate with the spin coater running at 1000 rpm.

Adsorption isotherms of epoxy resin and the curing agent on the chromate surface were obtained in the manner previously described[13,14] in order to assess the extent of interaction, at the most fundamental level, between the coating constituents and the substrates. Toluene was used as the casting solvent and the concentration of Epikote 828 and B002 were varied in the range 0.02–1.0 M. The adsorption samples were obtained by dipping 10 mm diameter discs of chromate treated steel in solutions of various concentrations followed by washing in toluene. A time dependent study was first carried out to establish the point of kinetic equilibrium, a time of 120 min for these adsorption experiments was thus chosen. These samples were investigated by monochromated Al-Kα XPS, high resolution spectra of C 1s were recorded for the epoxy resin samples and N 1s spectra for the curing agent. The C 1s peak for epoxy resin was resolved into its constituent components by peak fitting, and the epoxy resin uptake was calculated by using the intensity of the epoxy component of this spectrum. Curing agent uptake was calculated using the N 1s peak area.

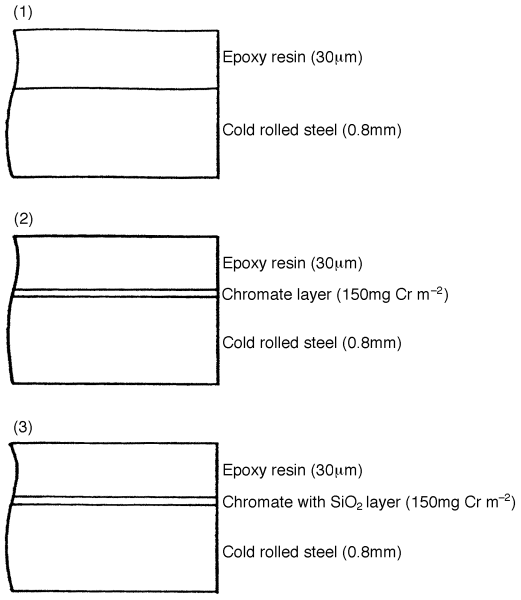

Fig. 1 Schematic representation of the three kinds of epoxy coated steel: (1) epoxy coated bare steel, (2) epoxy coated steel with chromate treatment, (3) epoxy coated steel with chromate + SiO_2

Cathodic delamination experiments

In keeping with previous cathodic delamination studies from this laboratory (*e.g.* ref. 15) experiments have been carried out using a 0.5 M NaCl solution at both an impressed cathodic potential of −1.5 V (*vs.* the saturated calomel electrode) and at the free corrosion potential (FCP), E_{corr}, of the metallic substrate. The reason for this is that at the FCP the exposed metal surface behaves as the anode and the coated steel, in particular the tip of the disbondment crevice, as the cathode. As coating delamination proceeds so the anodic region extends as the coating peels away from the substrate. This gradual extension of the anode leads to difficulties in the interpretation of the surface analysis data taken from interfacial failure surfaces. The solution to this dilemma, which has been employed in coatings research for the last two decades or so, is to polarise the metal substrate cathodically, at a well defined electrode potential. The value of −1.5 V is widely used, although alternative approaches involve the coupling of the coated metal to a zinc or aluminium anode. All have the same effect; the separation of anodic and cathodic sites and the consequential removal of the confusion regarding the exact position of such regions of electrode activity, which is crucial when using an area integrating technique, such as XPS, for surface analysis. Samples 20 mm × 100 mm of coated steel were prepared and the backs protected using Lacomite stopping off lacquer. After polarisation for the required time, the test was stopped and the extent of delamination was measured as described elsewhere.[15] The interfacial coating and substrate failure surfaces generated in this manner were then analysed by XPS.

Surface analysis by XPS and TOF-SIMS

X-Ray photoelectron spectra were recorded using a VG Scientific ESCALAB MKII system with a twin anode X-ray source (Al-Kα radiation was used in this investigation). The analyser was operated in the fixed analyser transmission (FAT) mode at a pass energy of 50 eV for the survey spectra and at 20 eV for high resolution spectra of the core levels of interest, the operating pressure was in the region of 10^{-9} mbar. The electron take off angle relative to the sample surface was 45° for most of the spectra recorded, but angle resolved XPS (with take-off angles of 15, 25, 35, 45, 60 and 90°) was used to investigate the initial chromate layer. Curve fitting of Cr 2p spectra was carried out by using the computer program developed by Proctor and included in his suite of programs entitled GOOGLY.[16] The curve fitting program uses an iterative non-linear least squares fitting method and allowed the operator to choose the background tail (the tail height to peak height ratio, referred to as the energy loss tail height or ELTH).[11] In this work, it is essential to consider the electron energy loss tail, because the chromate treatment has a layer structure. The base line can be fixed at zero and intercept can be unconstrained and is thus calculated by the program. The adsorption studies were carried out at RUST1, CLRC

Daresbury on a Scienta ESCA 300 spectrometer using monochromated Al-Kα radiation.

TOF-SIMS data were acquired using a VG Scientific Type 23 system. This instrument is equipped with a two-stage reflectron time of flight analyser and an MIG300PB pulsed liquid metal ion source. Static SIMS conditions were employed using a pulsed 30 keV $^{69}Ga^+$ primary ion beam rastered over an area 0.5 mm × 0.5 mm at 50 frames s^{-1}. Spectra were acquired over a mass range m/z 1–800 in both positive and negative ion modes. The mean molecular mass of chromium oxide was calculated from the TOF-SIMS data by the use of the following equation:

$$\sum\{m[I(Cr_nO_m)/\sum I(Cr_nO_m)]\}$$

where: m is the molecular mass of Cr-oxide and $I(Cr_nO_m)$ is the intensity of the specific Cr_nO_m fragment in the negative TOF-SIMS spectra.

Results and Discussion

Chemical composition of steel substrate and the chromate layers

The XPS survey spectra of chromate, chromate with SiO_2 treated steel and the bare steel substrate are shown in Fig. 2. The Cr 2p spectra are also shown and it is clear that there is a marked difference in the Cr^{6+}/Cr^{3+} ratio for the two treatments.

The chromate layers can be affected by X-ray irradiation during XPS analysis which may, conceivably, lead to the reduction of Cr^{6+} to Cr^{3+}. This possibility was investigated by time related acquisition of the Cr 2p spectra, and Fig. 3 shows the Cr 2p spectra of the chromate coating as a function

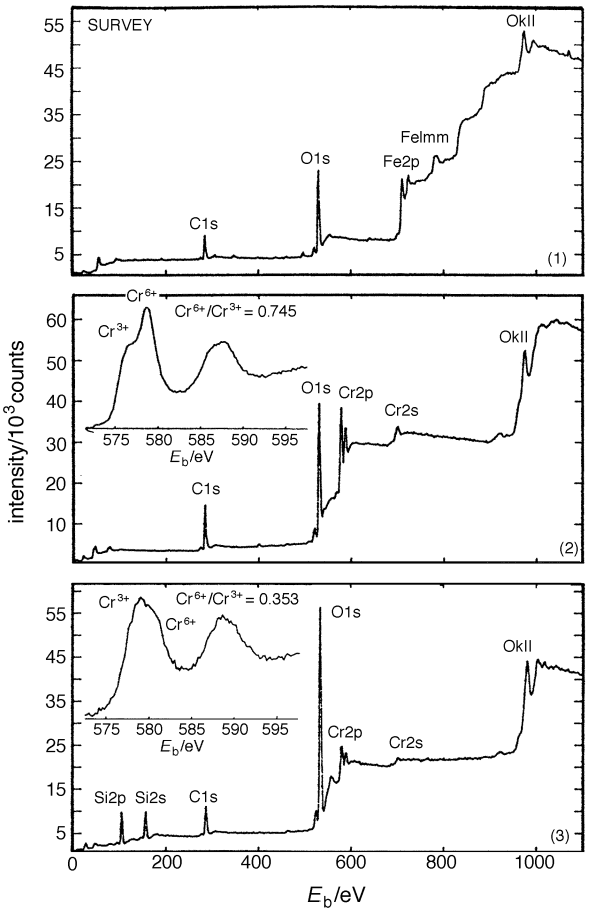

Fig. 2 XPS survey spectra and high resolution Cr 2p spectra of three kinds of pretreated surface before epoxy coating: (1) bare steel substrate, (2) chromate treated steel surface, (3) chromate with SiO_2 treated steel surface

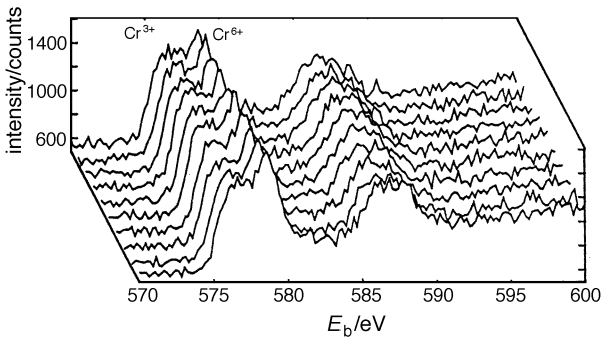

Fig. 3 High resolution Cr 2p spectra of chromate treated steel substrate under X-ray irradiation for 6 h

of X-ray radiation for times of up to 6 h, more than an order of magnitude longer than that usually employed for analysis. Little reduction of hexavalent to trivalent chromium was observed and it is thus safe to assume that differences in the Cr 2p spectra, which form an important part of this paper are not X-ray induced effects. The atomic ratio of trivalent/hexavalent chromium is evaluated by peak fitting of Cr 2p spectra considering Cr $2p_{3/2}$, Cr $2p_{1/2}$ and the shake-up satellite peaks as shown in Fig. 4. The positions of the shake-up satellites were set 9.5 eV higher than Cr $2p_{3/2}$ main peaks, 11 eV higher than Cr $2p_{1/2}$ main peaks, as indicated by Salvi *et al.*[17] The full width at half maximum (FWHM) of the hexavalent chromium component is 2.0 eV and that of the trivalent ion is 2.7 ± 0.1 eV. The XPS spectra recorded for the chromate + SiO_2 shows a degree (*ca.* 2 eV) of electrostatic charging as illustrated by the Cr 2p spectrum of this substrate in Fig. 4 which has not been corrected for electrostatic charging. This observation is potentially important as illustrates the insulating, or at best semi-conducting nature of the chromate + SiO_2 coating.

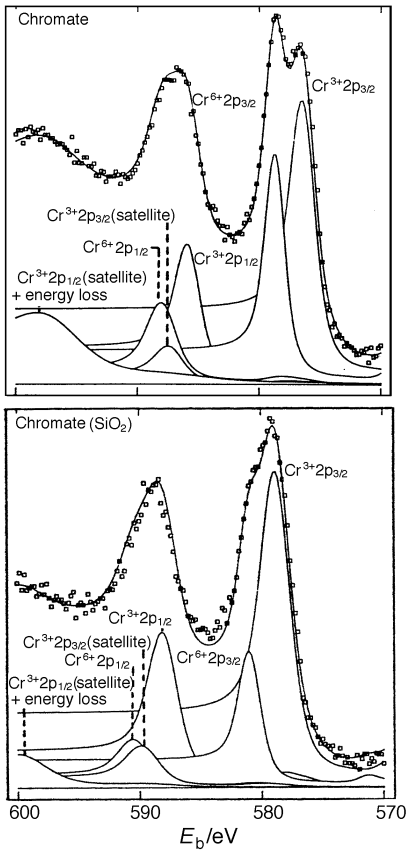

Fig. 4 The peak fitting results for the high resolution Cr 2p spectra of the chromate treated samples

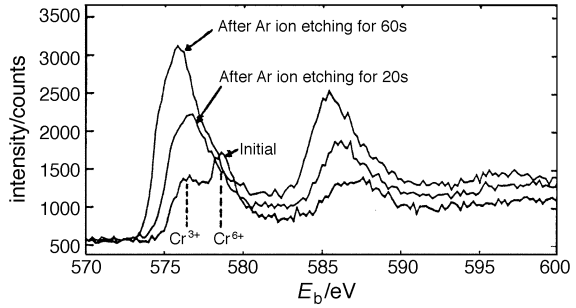

Fig. 5 High resolution Cr 2p spectra of the chromate treated steel following sputtering with argon ions

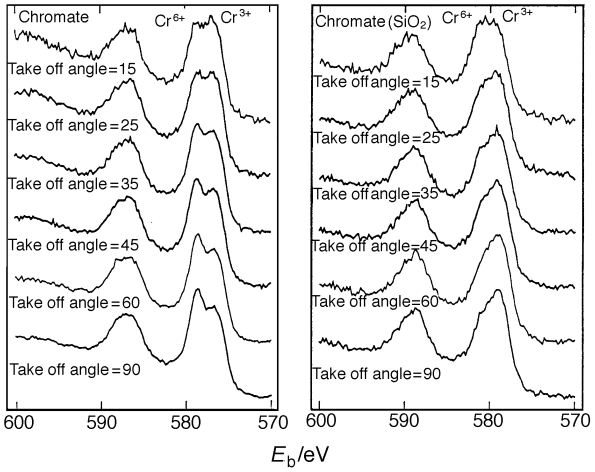

Fig. 6 High resolution angle resolved XPS: Cr 2p spectra of the chromate treated samples (take off angles are indicated on the spectra)

Compositional depth profile of the chromate layer by XPS

Argon ion sputtering is usually used for depth profiling, but there is the possibility of argon ion beam induced reduction of the Cr^{6+} species, the phenomenon is clearly seen in the spectra of Fig. 5. In order to circumvent this problem, angle resolved XPS was employed for the chromate treated samples. Fig. 6 shows the high resolution angle resolved Cr 2p XPS spectra for chromate and chromate/SiO_2 coatings. The Cr $2p_{3/2}$ binding energies of trivalent and hexavalent species are 577.8 and 580.5 eV, respectively. As the take off angle increases, so the intensity of the hexavalent chromium decreases for the chromate specimen, but increases for the chromate + SiO_2 coating. It was observed that the outer surface of the chromate + SiO_2 layer is Si rich compared with the composition of the chromate solution. The Si/Cr ratio of the outer surface was 5.6, but in the chromate solution with added SiO_2, the Si/Cr atomic ratio was 1.4. The chromate coating has clearly formed a layer structure on deposition on the steel substrate.

Chemical composition of the chromate layer by TOF-SIMS

The TOF-SIMS spectra of the chromate surface are shown in Fig. 7. Characteristic ions such as SiO_2^- ($m/z=60$), CrO_2^- ($m/z=84$), CrO_3^- ($m/z=100$) and others are expected from the chromate surfaces. Various chromium oxide assignments were made in the TOF-SIMS spectra ($m/z=1$–800) such as Cr_nO_m ($n=1$–10, $m=n+1$–$3n$). The spectra also contained, in the case of the chromate + SiO_2 layer, signals attributable to $SiOH^-$ ($m/z=61$), CrO_2H^- ($m/z=85$), CrO_3H^- ($m/z=101$) and so on, which implies the presence of surface silanol groups and hydrated silicon and chromium species. This observation is supported by the determination of the Si Auger parameter. This can be achieved in conventional XPS by the use of the Bremsstrahlung radiation from a twin anode X-ray source to excite the Si KLL Auger transition at a kinetic energy of *ca.* 1610 eV.[18] The Si Auger parameter in this case is simply the summation of the Si 2p photoelectron peak binding energy and the Si KLL kinetic energy. An Auger parameter of 1711.5 eV was determined, this value is similar to that of SiO_2 gel and indicates that the surface Si is hydrated. These surface silanol groups and the hydrated silicon and chromium oxides may provide sites for good adhesion. The mean chromium oxide molecular mass was calculated to be 204 u for the initial chromate surface and 143 u for the initial chromate with SiO_2 surface. The chromium oxide molecular mass of the chromate + SiO_2 treatment is therefore substantially lower than that of the plain chromate treatment. It is considered that SiO_2 particles reduce the extent of cross-linking amongst the chromate 'oxide' species. The TOF-SIMS spectra of the outer surface for chromate with SiO_2 layer reveal little, if any, evidence of a chemical interaction between the chromium oxide species and the colloidal SiO_2. After 60 s continuous ion erosion using the same ion source, the TOF-SIMS spectrum of chromate with SiO_2 layer is noticeably different from that of the chromate layer with a clear signal discernible at $m/z=$ 288 which could be attributable to $Cr_4O_5^-$ or $Cr_2SiO_8^-$. The spectra of both the chromate inner layers after such ion etching are shown in Fig. 8. The spectrum of the plain chromate layer is almost the same as the initial surface, but that of chromate + SiO_2 has evolved quite significantly. The spectrum of chromate + SiO_2 has signals in the negative ion spectrum at $m/z=144$ ($CrSiO_4^-$), 160 ($CrSiO_5^-$), 204 ($CrSi2O_6^-$), all of which arise from the complexation of the colloidal SiO_2 and the chromate layer. This result indicates that the inner region of the chromate + SiO_2 layer has a complex cross-linked structure which consists of SiO_2 and Cr oxide compared with the plain chromate layer inner zone which is thought to be a higher molecular mass Cr^{6+} and Cr^{3+} region.

Adsorption properties of the chromate layer

It is well known that there can be hydrogen bonding between epoxy resin and steel surface. Such bonding has little resistance against water and alkaline environments. Interfacial failure is often observed for bare steel samples exposed to cathodic conditions (see for example ref. 4 for a discussion of this point). It is thought that the specific bonds formed between the chromate layer and the epoxy resin are stronger than those between the bare steel and the epoxy as failure of the chromate inner layer was observed for chromate samples. To gain further insight regarding the interfacial characteristics of the thin film samples of the chromate coated with the epoxy resin were prepared, and investigated by XPS. Fig. 9 shows the high resolution C 1s spectra of spin coated samples on the two types of chromate substrates and resin bulk. These results show that the interfacial region between resin and substrate was different from the bulk. This provides further, direct, evidence of specific interfacial interactions leading to good adhesion between the coating and the substrate. There is evidence within the C 1s spectra of Fig. 9 that the intensity of the epoxy component (at a binding energy of *ca.* 286.6 eV) is reduced slightly as well as shifting to a slightly higher binding energy. This is indicative of the opening of the strained epoxy ring on interaction with the substrate and perhaps an interaction of the remaining epoxy groups with the chromated steel surfaces. The shift to a higher binding energy is certainly consistent with increased electron-withdrawing behaviour on the formation of the organic–inorganic bond.[12] This component of the C 1s spectrum is used in the adsorption isotherm studies described below, and the reduction in epoxy intensity compared with the bulk resin clearly provides a potential source of error. The use of this component in the adsorption isotherms is justified, however, as the changes in the spectra are consistent between substrate types.

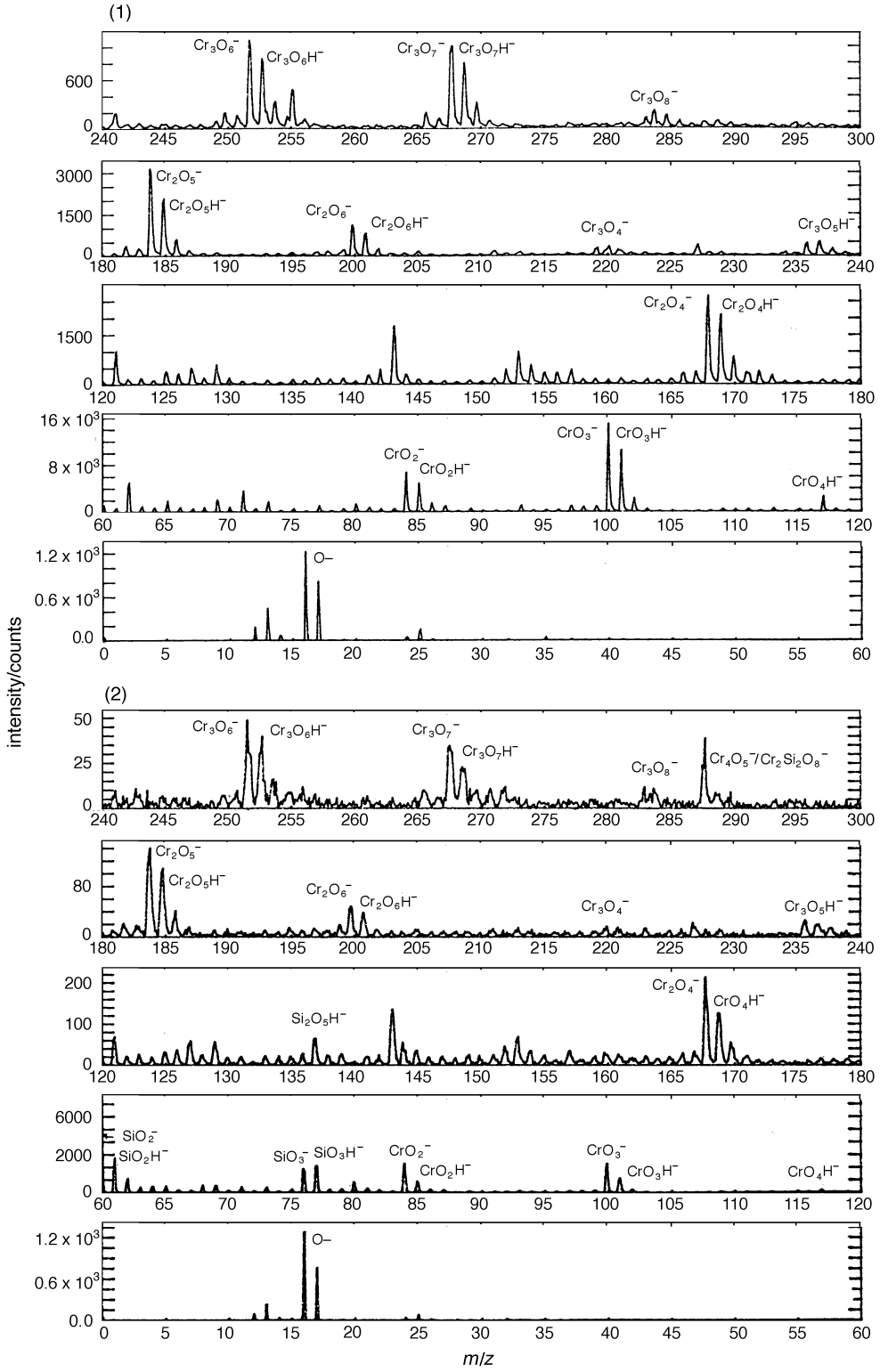

Fig. 7 The negative TOF-SIMS spectra of (1) chromate initial surface, and (2) chromate + SiO_2 initial surface

The adsorption isotherms obtained in this manner may conform to the Langmuir equation[13]

$$S/y = 1/(BX_m) - S/X_m$$

where: S is the solution concentration, y is the uptake measured by XPS (atom%), X_m is the monolayer coverage and B is a constant, $[A \exp(-\Delta H_{ads}/RT)]$, where ΔH_{ads} is the heat of adsorption.

This class of adsorption is confirmed by the Langmuir plots of Fig. 10 and 11 which show the adsorption characteristics of the epoxy resin and the curing agent on the chromate surfaces. The relationship between S/y and S is linear which indicates Langmuir adsorption, and allows monolayer coverage to be calculated in each case. Both values of X_m for the epoxy resin and the curing agent on chromate are greater than that defined on the chromate + SiO_2. This indicates that the chromate surface has more suitable bonding sites than chromate + SiO_2 surface. Generally, the more bonding sites that are available, the better the coating durability. One of the major assumption in the Langmuir equation is that the heat of adsorption is constant during monolayer development. That is to say that it is not influenced by either the proximity of adsorbed species

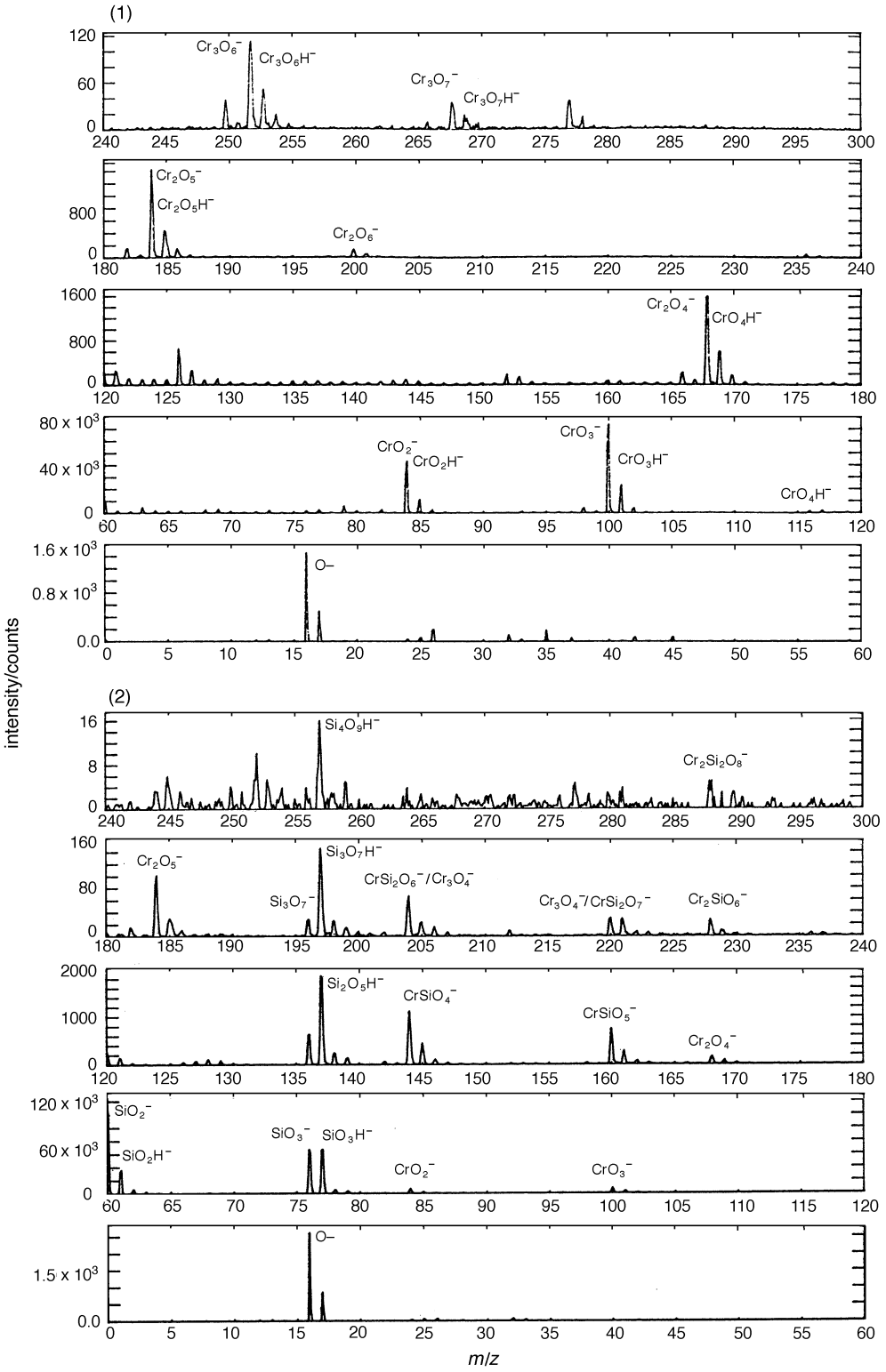

Fig. 8 The negative TOF-SIMS spectra of chromate layer after 1 min ion etching: (1) chromate layer, (2) chromate + SiO_2 layer

or the type of bonding site, which are all deemed to be equivalent. This latter point brings us to the rather surprising conclusion that, in the case of the chromate + SiO_2 layer, there is no difference in adsorption characteristic of either molecule on 'chromate' or 'SiO_2' sites. They are, if they do indeed exist as discrete sites, energetically equivalent from an adsorption point of view. The results indicate the number of available sites for bonding is greater on the chromate substrate than the chromate + SiO_2. One must recall, however, that this analysis makes no distinction between bond strength. It would be perfectly feasible, for example, for the chromate + SiO_2 treatment to confer better durability by virtue of stronger interfacial interactions. The C 1s spectra of Fig. 9 do, indeed, imply this as the epoxy group (*ca.* 286.6 eV) has shifted to a slightly higher binding energy in the case of this substrate.

Kinetics of cathodic delamination

Table 1 shows the cathodic delamination rates for the three epoxy coated steel substrates. These results show that the chromate treatment provides good coating durability under immersed condition at both the impressed cathodic potential

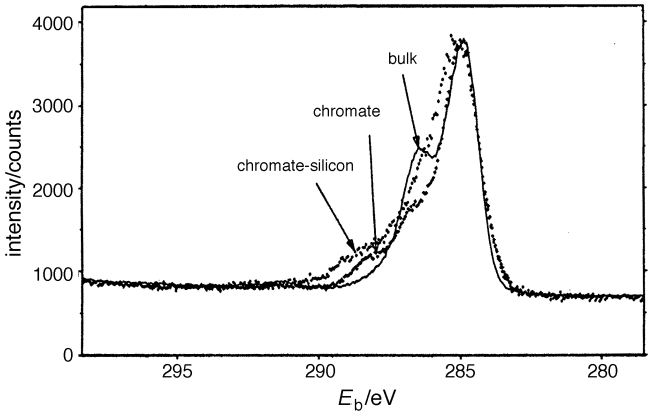

Fig. 9 High resolution C 1s spectra of epoxy resin bulk (thick layer) and spin-coated chromate samples where the polymer/substrate interfacial chemistry is probed directly by monochromated Al-Kα XPS

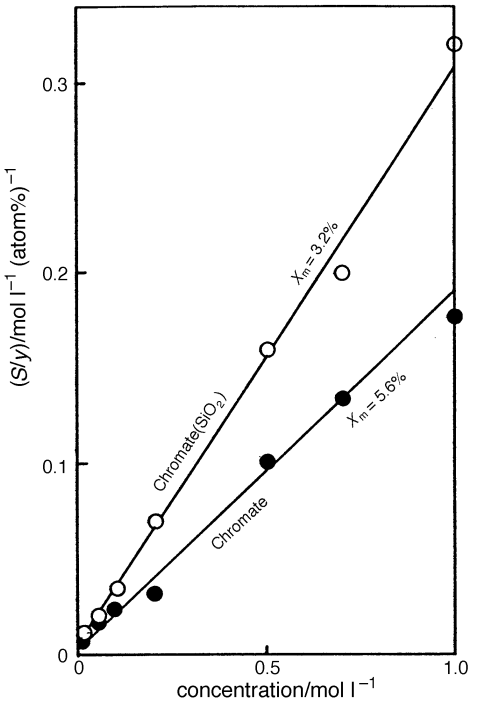

Fig. 10 Lamgmuir plots of epoxy resin on chromate treated samples

and E_{corr}. It is well known that a cathodic potential will accelerate coating delamination. So these results, showing that the delamination rate is larger at the cathodic potential than at the free corrosion potential, are expected and in agreement with previous work.[19] However, the relative delamination rates at a cathodic potential and the free corrosion potential were qualitatively the same within each set of three samples. To understand the degradation mechanism of these coated steel panels, it is necessary to consider the electrochemical reactions that occur at the exposed metal surface. The outer edges of the samples will be anodic at free corrosion potential, whereas the region under coating will be cathodic. The following reactions will occur at the anode and cathode.

$$\text{anodic reaction: } Fe \rightarrow Fe^{2+} + 2e^-$$

$$\text{cathodic reaction: } 1/2O_2 + 2H_2O + 4e^- \rightarrow 2OH^- \ [\leftarrow Na^+{}_{aq}]$$

The other cathodic reaction that will occur at the impressed cathodic potential, is as follows.

$$\text{cathodic reaction: } 2H_2O + 2e^- \rightarrow H_2\uparrow + 2OH^- \ [\leftarrow Na^+{}_{aq}]$$

In both cases the Na^+ ion from solution will act as a marker

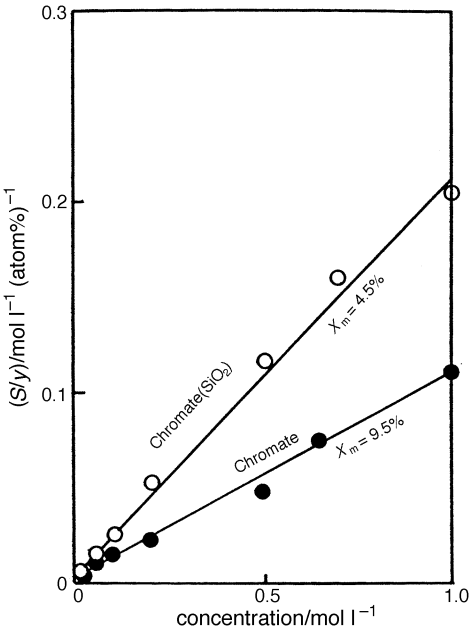

Fig. 11 Langmuir plots of curing agent on chromate treated samples

Table 1 Delamination kinetics of various surface treatments

sample	immersion at E_{corr}/ mm day^{-1}	immersion at -1500 mV/ mm day^{-1}
bare steel	10.0	20.0
chromate treatment	2.2	10.0
chromate + SiO_2 treatment	0.1	1.5

for cathodic behaviour which is retained on removal of the sample from the test solution.

XPS analysis of the interfacial failure surfaces

XPS analysis was undertaken on the interfacial failure surface of three kinds of samples after the delamination tests. The XPS survey spectra of the bare steel, chromated steel and chromate + SiO_2 steel failure interface is shown in Fig. 12, 13 and 14, respectively. Table 2 shows the quantitative surface analysis obtained by XPS. The spectra all show peaks associated with carbon, oxygen, nitrogen, sodium, chloride, silicon (for the chromate + SiO_2 specimen), iron and chromium. The carbon levels present on all interfacial metal surfaces are low (generally $\lesssim$30 atom%) which is indicative of the true interfacial failure characteristic of cathodic delamination.[20,21] The high resolution Cr 2p spectra (inset in Fig. 12–14) show that there are differences in interfacial failure chromium chemistry for the two chromate treatments. The sodium concentrations are 5–15 atom% while those of chlorine are 0–2.4 atom%. The sodium has diffused through the coating and along the developing disbondment crevice between the steel substrate and coating and acts as a counter-ion for the OH^-, which has been produced by the cathodic reaction at the interface. Indeed, it is well established that the presence of a cationic marker such as this, identified by surface analysis methods, acts as a marker for the prior electrochemical history of an electrode surface.[22] In this case it is clear that cathodic conditions do indeed exist within the extending failure crevice for both the cathodically polarised panels and those at the FCP. This is in complete agreement with previous, extensive work, on the phenomenon of cathodic delamination from this laboratory.[6]

Interfacial analysis of the chromate treated steel samples indicate that failure has occurred within the chromate coating. The metal and resin side of the delaminated interface both

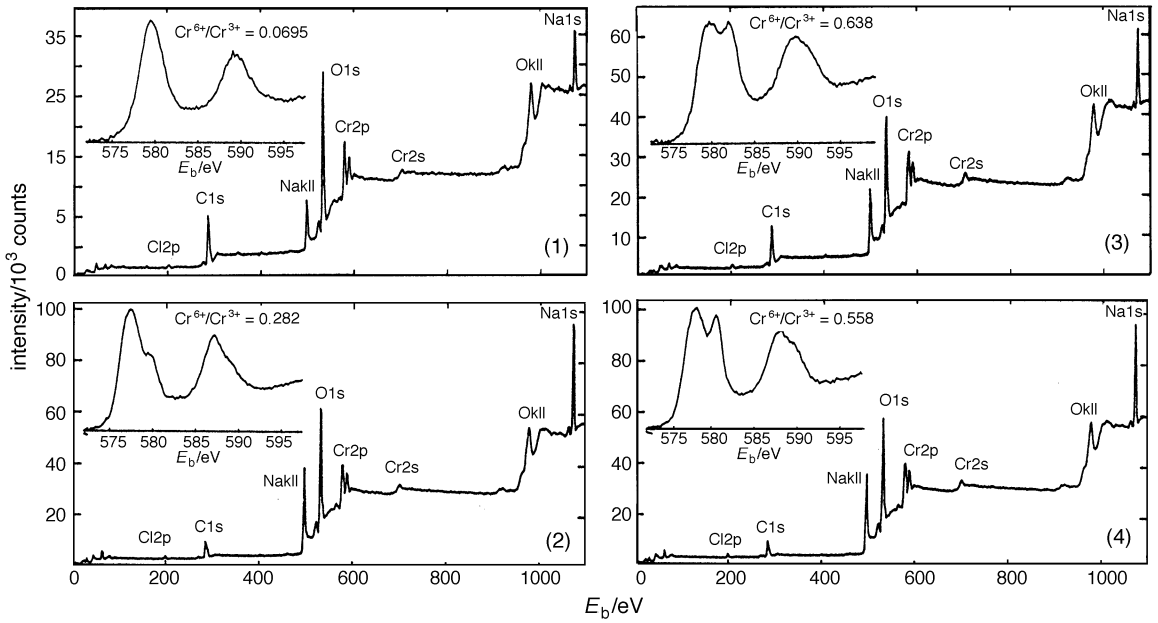

Fig. 12 Survey spectra and high resolution Cr 2p spectra of the interfacial failure surfaces of epoxy coated steel with chromate treatment. (1) Epoxy side, −1.5 V *vs.* SCE, (2) steel side, −1.5 V *vs.* SCE, (3) epoxy side, E_{corr}, (4) steel side, E_{corr}.

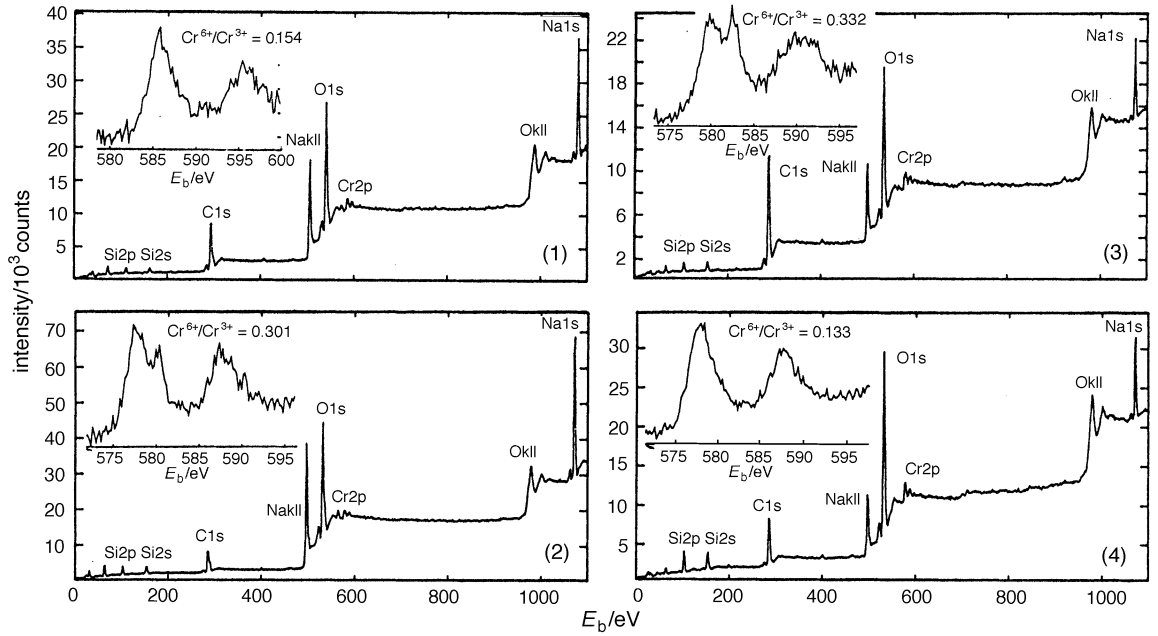

Fig. 13 Survey spectra and high resolution Cr 2p spectra for interfacial failure surfaces of epoxy coated steel with chromate + SiO_2 treatment. (1) Epoxy side, −1.5 V *vs.* SCE, (2) steel side, −1.5 V *vs.* SCE, (3) epoxy side, E_{corr}, (4) steel side, E_{corr}.

show very high chromium signals for the chromate and the chromate + SiO_2 pretreatments. The latter spectra have a very high Si concentration, supporting the concept of inner chromate layer failure as shown in Fig. 15. The case for the bare steel substrates is, however, somewhat different. Both failures at FCP and the cathodically polarized tests, show the low concentration of carbon and well defined Fe 2p transition, centred at *ca.* 710 eV, associated with classical cathodic delamination reported before. These results do, however, provide a useful bench mark against which to assess the failure of the conversion coated samples. Fig. 16 shows a TOF-SIMS image of the resin side interface for a bare steel sample treated at the cathodic potential. The result indicates that there is an island-like distribution of iron on the epoxy resin side of the failure. It is thought that the dissolution of iron oxide occurs following interfacial separation and is then adsorbed on the underside of the epoxy resin coating as indicated in the schematic of Fig. 15. This behaviour is predicted from the Pourbaix (electrode potential: pH) diagram for iron,[23] at high pH (>14) and at a cathodic potential less than −1200 mV. Thus it is a viable and likely scenario for the cathodically polarised specimens, but is unlikely to occur in the case of those at the free corrosion potential. In the latter case the presence of any iron on the underside of the polymer can be assigned to the back deposition of corrosion product from solution. The high resolution Cr 2p spectra for chromate samples show that the ratio of Cr^{6+}/Cr^{3+} reduced after delamination compared with initial values for both treatments. This indicates that the reduction of hexavalent chromium to trivalent chromium as a result of the underfilm cathodic conditions has occurred. Fig. 17 shows the Cr 2p spectra of uncoated chromate samples after exposure to 0.5 M NaCl aqueous solution and distilled water for 20 min. These results also show that the ratio of Cr^{6+}/Cr^{3+} was also reduced. The change of this ratio for the specimen treated in 0.5 M NaCl

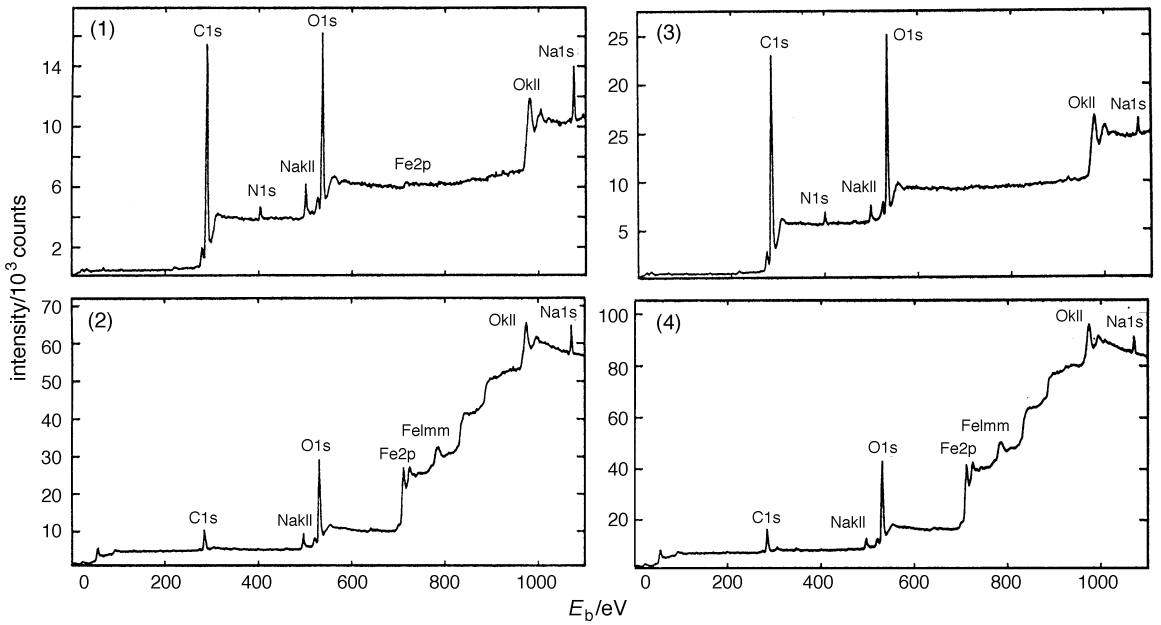

Fig. 14 Survey spectra and high resolution Cr 2p spectra of interfacial failure surface of epoxy coated bare steel. (1) Epoxy side, −1.5 V *vs.* SCE, (2) steel side, −1.5 V *vs.* SCE, (3) epoxy side, E_{corr}, (4) steel side, E_{corr}.

Table 2 Results of quantitative XPS for various delaminated interfaces (atom%)

samples	test condition	C	O	Cr	Na	Cl	Si	Fe	N	Cr^{6+}/Cr^{3+}
bare steel	initial	35.9	54.3					9.7		
	E_{corr} steel	39.0	48.3		2.1	1.3		9.7		
	E_{corr} resin	77.1	19.0		1.0				2.6	
	−1500 mV steel	30.5	53.5		5.2			9.7	1.4	
	−1500 mV resin	73.4	20.1		2.5			1.0	2.6	
chromate	initial	35.0	52.6	12.3						0.745
treatment	E_{corr} steel	21.5	52.0	9.3	14.7	2.4				0.558
	E_{corr} resin	38.5	41.0	7.8	9.1	2.0			1.5	0.638
	−1500 mV steel	23.3	52.5	7.9	15.5	1.2				0.282
	−1500 mV resin	43.2	42.3	6.0	6.7	1.3			0.6	0.070
chromate	initial	24.6	52.2	3.5			19.7			0.353
$+SiO_2$	E_{corr} steel	33.6	43.9	3.5	5.0	0.5	13.0			0.133
treatment	E_{corr} resin	57.4	29.8	1.8	5.1		4.4		1.6	0.332
	−1500 mV steel	24.2	48.0	1.7	17.5	0.6	8.0			0.301
	−1500 mV resin	38.3	40.7	1.2	12.7	0.5	5.3		1.3	0.154

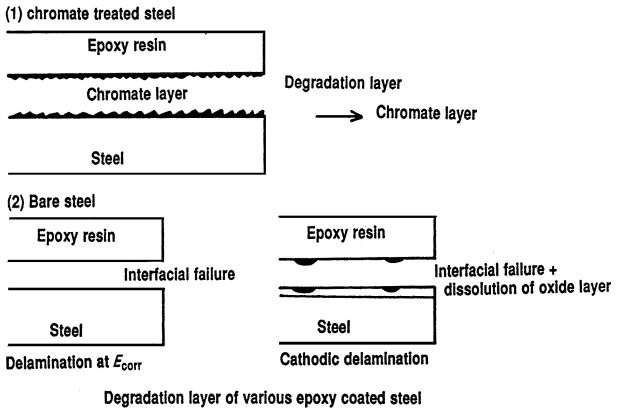

Fig. 15 Schematic view of degradation of the interfacial layers of the various samples

solution was considered to be a result of the occurrence of the localised cathodic reaction on chromate substrate, in distilled water dissolution of the Cr^{6+} ion from the substrate, is thought to be more likely. Additional experiments to confirm this result were carried out by adjusting the pH of the saline solution with NaOH. The reduction in the Cr^{6+}/Cr^{3+} ratio of the chromate surface after dipping NaCl solutions of varying pH is shown in Fig. 18. The higher the pH of the solution the greater the reduction in the Cr^{6+}/Cr^{3+} ratio, particularly above pH = 12. This is analogous to the situation that exists under the coating, at the crevice tip, during delamination. The cathodic reaction causes the development of a high pH environment, and as Cr^{6+} is more soluble, the cross-linked structure is destroyed and coating delamination occurs, with a residue of the chromate layer on both interfacial surfaces. It is clear, therefore, that the changes in the Cr^{6+}/Cr^{3+} ratio were caused by the cathodic reaction and the dissolution of the Cr^{6+} component of the pretreatment coating. Under the coating (at the very tip of the disbondment crevice) it was not possible for Cr^{6+} ions to permeate through the coating, or the path between coating and substrate because of the large radius of the hydrated ion. So the changes of the chromate layer were caused, predominantly, by the Cr^{6+} reduction reaction (cathodic reaction). According to the Pourbaix diagram for Cr,[23] Cr^{3+} is more stable than Cr^{6+} at high pH and cathodic potentials. The model of the non-rinse chromate layer that has been proposed is a cross linked structure which consisted of Cr^{6+} and Cr^{3+}. Cathodic reduction reaction of hexavalent to trivarent chromium destroys this cross linked structure of the chromate layer as shown in Fig. 19.

Further evidence for the degradation of this cross-linked structure is obtained from the TOF-SIMS analysis from failure

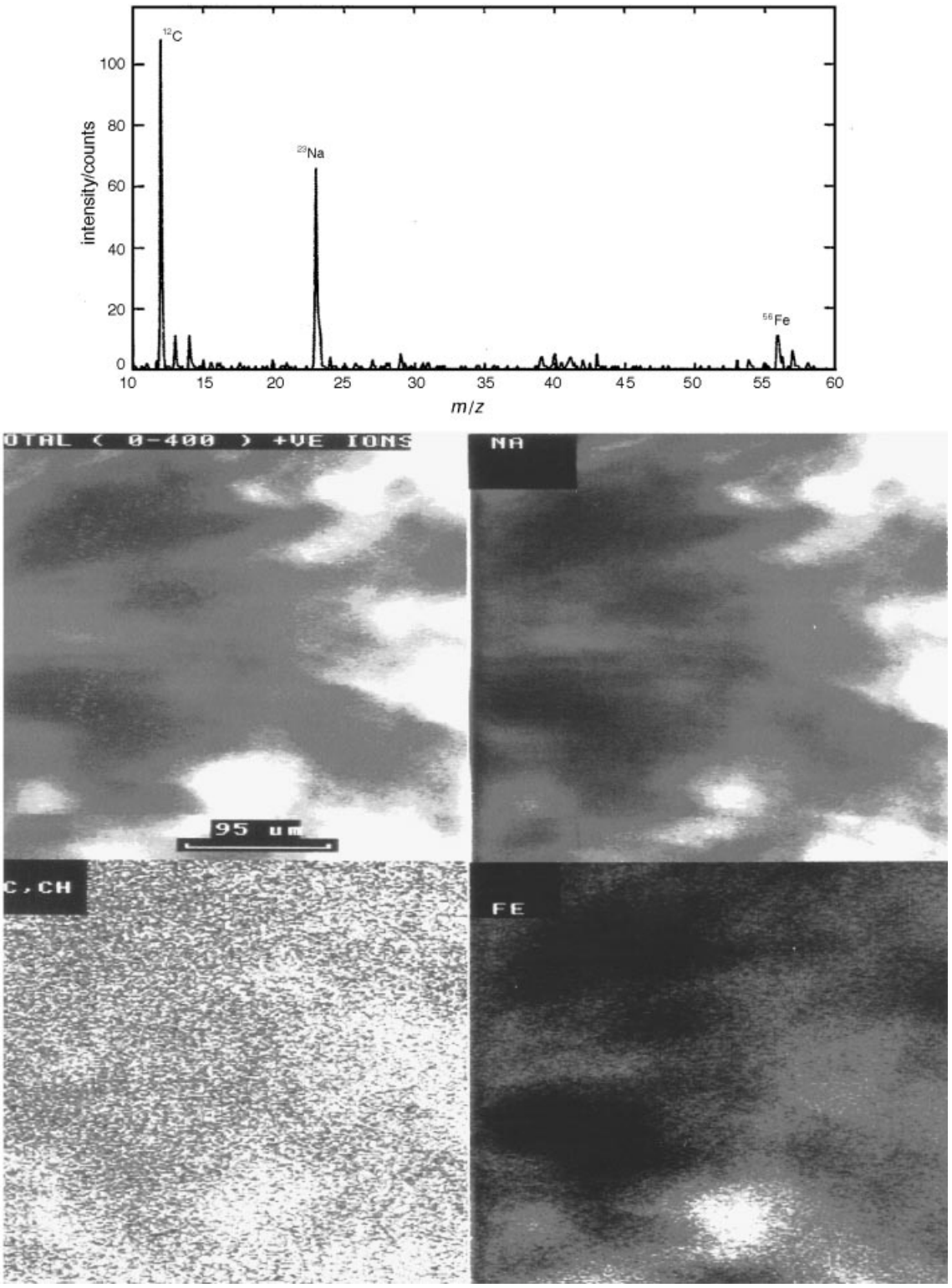

Fig. 16 Results of TOF-SIMS (positive ions) and imaging TOF-SIMS for resin side delamination interface of epoxy coated steel at −1.5 V *vs.* SCE

interfaces and the uncoated specimens exposed to saline solutions of increasing pH. Fig. 20 shows the relationship between Cr^{6+}/Cr^{3+} ratio and mean chromium oxide molecular weight calculated from the TOF-SIMS data for the metal interfacial failure surface and the chromate surfaces exposed to 0.5 M NaCl solutions. These results support the hypothesis that the cross-linked structure of the chromate layer is destroyed by exposure to cathodic conditions. The chromate + SiO_2 treated samples have relatively good durability compared with the plain chromate treated sample because the colloidal SiO_2 has adsorbed Cr^{3+} and this acts as a barrier protecting the layer against degradation from factors such as hydroxyl ions. The chromate + SiO_2 treated layer is not conductive (electrostatic charging is observed in the high resolution XPS spectra). This layer acts as a barrier for not only oxygen, water and cations, but also for electrons. It is thought that the non-conductive property controls the rate of reaction at the cathodic site and contributes to the good adhesion durability compared with the plain chromate treated sample, which has better conductivity. Additionally, the cathodic reaction for the chromate + SiO_2 treated sample will occur more easily at the inner chromate layer near the steel/chromate interface than at the outer surface of the chromate layer, as indicated in Fig. 21. On the other hand, the cathodic reaction for the plain chromate

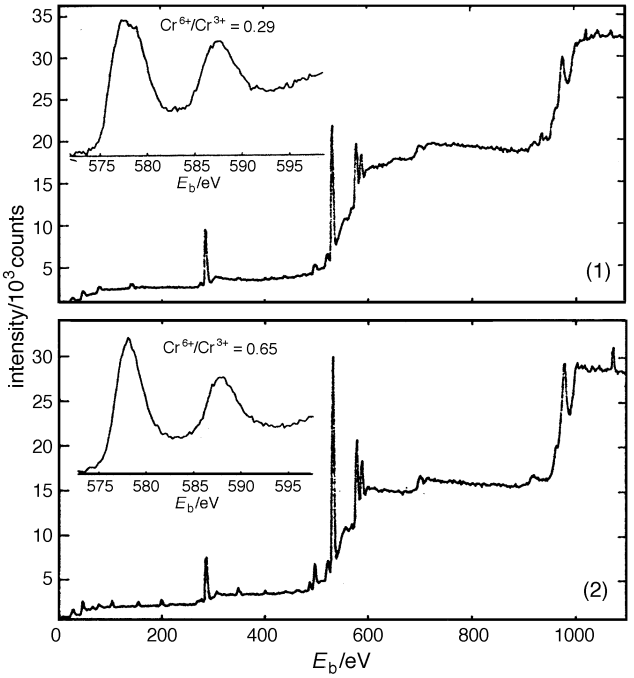

Fig. 17 Survey spectra and high resolution Cr 2p spectra of chromate treated steel substrate immersed in (1) 0.5 M NaCl aqueous solution, and (2) distilled water

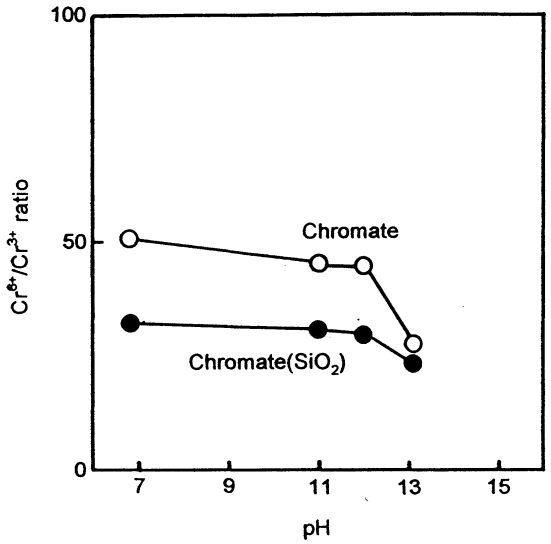

Fig. 18 The effect of solution pH on the Cr^{6+}/Cr^{3+} ratio of chromate surfaces

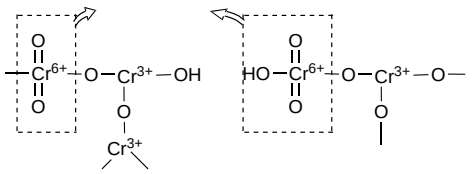

Fig. 19 Chromate layer structure and the degradation of the chromate layer

sample will occur at the inner chromate layer near the outer surface of the chromate. In contrast to the chromate+SiO_2 treatment this deposit has a layer structure in which Cr^{6+} is richer at the inner chromate layer than at the outer surface. The inner layer, which is rich in Cr^{6+}, is more easily destroyed by the cathodically generated alkali than the outer chromate surface. This is shown schematically in Fig. 21.

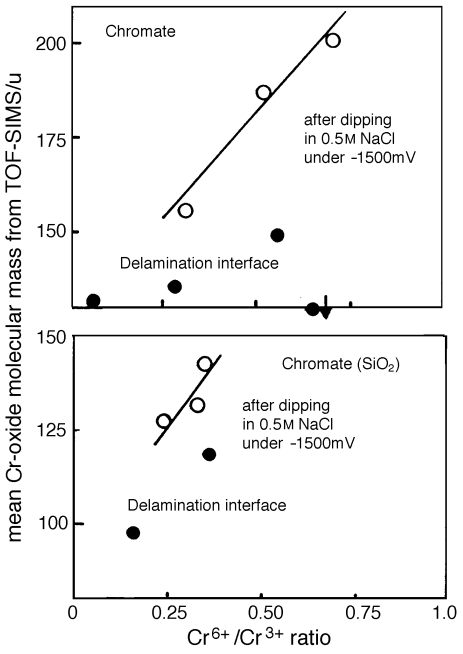

Fig. 20 The relationship between Cr^{6+}/Cr^{3+} ratio and mean Cr oxide molecular mass for the chromate and chromate+SiO_2 surfaces after immersion in 0.5 M NaCl at -1.5 V *vs.* SCE

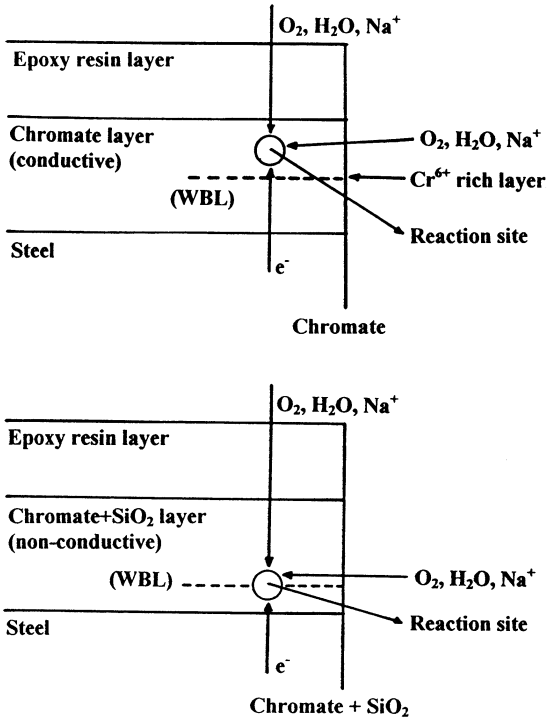

Fig. 21 The schematic view of the proposed degradation mechanism for the two types of chromate pre-treatments

These cathodic reactions can occur as result of aggressive species such as water and oxygen, together with electrons, the oxygen permeating through the coating layer. Other reactions are possible, for example, the direct reduction reaction in the chromate layer as follows.

cathodic reaction:

$$CrO_4^{2-} + 4H_2O + 3e^- \rightarrow Cr(OH)_3 + 5OH^- \; [\leftarrow Na^+_{aq}]$$

Cr^{3+} is more stable than Cr^{6+} under cathodic and alkaline conditions.[23] If there are cathodic regions under the coating, then cathodic reduction reactions will occur. These cathodic reactions cause an increase in the concentration of OH^- under

the epoxy coating layer and causes destruction of chromium oxide structure.

There is also the possibility that the paint film may act as an ion exchange membrane which will have a marked effect on the arrival of cations through the coating although not along the developing cathodic crevice. There have been attempts to model the transport properties of ionic species within paint films (see, for example the elegant mathematical treatment of Ruggeri and Beck[24]), but the necessary ionic transfer numbers are not, to our knowledge, available for the amine cured epoxy used in the present investigation. It is interesting to note that in work with an amine cured epoxy powder coating of some 350 μm in thickness, Watts and Castle[20] were able to show that electrical neutrality was maintained across the thickness of a disbonding coating. The excess of sodium cations present at the interfacial failure surface was complemented by an excess of chloride anions at the outer surface. It is well established, however, that the cathodic delamination of an organic coating from a pre-existent defect or exposed edge of a metal substrate does not require, *per se* the presence of the cationic species.[19] The ion exchange properties of the paint film may, however, play an important role in the development of the initial defect. This situation is not considered in this work as the exposed metal surface would always act as the active electrode, as it does in all cathodic delamination test procedures.

Conclusions

The use of XPS and TOF-SIMS provides valuable information concerning the coating delamination of various samples.

1 The chromate layer on steel substrate has a cross-linked structure which consists of Cr^{3+} and Cr^{6+} for the chromate treatment and Cr^{3+}, Cr^{6+} and SiO_2 for chromate + SiO_2 treatment. In the inner layer of the chromate + SiO_2 treatment there is bonding between the Cr oxide and the SiO_2, and a more complex structure than for the plain chromate layer.

2 For the chromate treatment, Cr^{3+} is enriched at the substrate, but for chromate + SiO_2, Cr^{6+} and SiO_2 are richer at the substrate.

3 The chromate surface contains hydrated Cr oxide and the chromate + SiO_2 surface has hydrated Cr oxide, together with silanol groups and hydrated silicon species. These substrates show good adhesion with the organic resin. The results of adsorption isotherm of epoxy resin and curing agent have shown that the chromate layer has more bonding sites than the chromate + SiO_2. Thus the chromate provides many adsorption sites for the organic molecules, although the bonds formed with the chromate + SiO_2 may be stronger. Both will enhance the resistance of a steel substrate to cathodic delamination.

4 The kinetics of cathodic delamination for the three epoxy coated steel substrates ranked as follows: bare steel > chromate steel > chromate with SiO_2 steel, for exposure to saline solution at both an impressed cathodic potential and E_{corr}.

5 There was a high concentration of sodium at the delaminated interface at both free corrosion potential and a large cathodic potential. This shows the delamination surface to be a strong cathode and that the cathodic reaction to produce OH^- has occurred.

6 The delamination interfaces for chromate and chromate + SiO_2 were located at the inner chromate layer at both potentials. The failure of bare steel was interfacial at E_{corr} and interfacial with inorganic layer dissolution at -1.5 V.

7 The Cr^{6+}/Cr^{3+} ratio changed during delamination. This is the result of Cr^{6+} dissolution into aqueous solution and the cathodic reduction reaction of Cr^{6+} to Cr^{3+} under the coating.

8 The cross-linked structure is destroyed by the dissolution of the Cr^{6+} component in a high pH environment at the cathodic potential. This layer becomes a weak boundary layer the failure of which causes delamination.

The authors wish to thank S. J. Greaves and A. M. Brown at University of Surrey for help with the use of XPS and TOF-SIMS respectively.

References

1 Y. Yoshikawa and J. F. Watts, *Surf. Interface Anal.*, 1993, **20**, 379.
2 J. A. Treverton and A. Bosland, *Corrosion Sci.*, 1995, **37**, 723.
3 A. M. Taylor, J. F. Watts, J. Bromley-Barratt and G. Beamson, *Surf. Interface Anal.*, 1994, **21**, 697.
4 J. F. Watts, in *Problem Solving Methods in Surface Analysis*, ed. J. C. Riviere and S. Myhra, Marcel Dekker Inc., New York, 1998, to be published.
5 R. A. Dickie, L. P. Haak, J. Jethwa, A. J. Kinloch and J. F. Watts, *J. Adhesion*, in press.
6 J. F. Watts, *J. Adhesion*, 1989, **31**, 73.
7 J. E. Castle, in *Proc. Corrosion '97, vol. 2: Corrosion Resistant Coatings*, NACE, Houston TX, 1997, pp. 165–175.
8 J. F. Watts and J. E. Castle, *J. Mater. Sci.*, 1983, **18**, 2987.
9 J. F. Watts, J. E. Castle and S. J. Ludlam, *J. Mater Sci.*, 1986, **21**, 2965.
10 J. E. Castle, in *Organic Coatings*, ed. P. C. Lacaze, AIP Conference Proceedings, American Institute of Physics, 1995, vol. 354, pp. 432–449.
11 J. E. Castle, R. Ke and J. F. Watts, *Corrosion Sci.*, 1990, **30**, 791.
12 S. R. Leadley and J. F. Watts, *J. Adhesion*, 1997, **60**, 175.
13 C. A. Baillie, J. F. Watts and J. E. Castle, *J. Mater. Chem.*, 1992, **2**, 939.
14 M. L. Abel, M. M. Chehimi, A. M. Brown, S. R. Leadley, and J. F. Watts, *J. Mater. Chem.*, 1995, **5**, 845.
15 J. E. Castle and J. F. Watts, *Ind. Eng. Chem. Prod. Res. Develop.*, 1985, **24**, 361.
16 J. N. Feidor, A. Proctor, M. Houalla and D. M. Hercules, *Surf. Interface Anal.*, 1993, **20**, 1. Full details of fitting procedures obtained from: A Proctor, TRYFIT and GOOGLY Manuals supplied to the University of Surrey.
17 A. M. Salvi, J. E. Castle, J. F. Watts and E. Desimoni, *Appl. Surf. Sci.*, 1995, **90**, 333.
18 R. H. West and J. E. Castle, *J. Electron Spectrosc.*, 1980, **18**, 355.
19 J. F. Watts, J. E. Castle, P. J. Mills and S. A. Heinrich, in *Corrosion Protection by Organic Coatings*, ed. M. W. Kending and H. Leidheiser Jr., The Electrochemical Society, Pennington, NJ, 1987, p. 68.
20 J. F. Watts and J. E. Castle, *J. Mater. Sci.*, 1984, **19**, 2259.
21 S. J. Davis and J. F. Watts, *J. Mater. Chem.*, 1996, **6**, 479.
22 J. E. Castle and D. C. Epler, *Surf. Sci.*, 1975, **53**, 286.
23 *Encyclopedia of Electrochemistry of the Elements*, ed A. J. Bard, Marcel Dekker Inc., New York., 1986, vol. 9.
24 R. T. Ruggeri and T. R. Beck, in *Corrosion Control by Organic Coatings*, ed. H. Leidheiser Jr., NACE, Houston TX, 1981, pp. 62–69.

Paper 7/08929E; *Received* 11*th December*, 1997